Spectroscopic analysis of the open 3*d* subshell transition metal aluminides: AlV, AlCr, and AlCo

Jane M. Behm,[a] Dale J. Brugh, and Michael D. Morse
Department of Chemistry, University of Utah, Salt Lake City, Utah 84112

(Received 9 May 1994; accepted 28 June 1994)

Three open 3*d* subshell transition metal aluminides, AlV, AlCr, and AlCo, have been investigated by resonant two-photon ionization spectroscopy to elucidate the chemical bonding in these diatomic molecules. The open nature of the 3*d* subshell results in a vast number of excited electronic states in these species, allowing bond strengths to be measured by the observation of abrupt predissociation thresholds in a congested optical spectrum, giving $D_0^0(\mathrm{AlV})=1.489\pm0.010$ eV, $D_0^0(\mathrm{AlCr})=2.272\pm0.009$ eV, and $D_0^0(\mathrm{AlCo})=1.844\pm0.002$ eV. At lower excitation energies the presence of discrete transitions has permitted determinations of the ground state symmetries and bond lengths of AlV and AlCo through rotationally resolved studies, giving r_0'' (AlV, $\Omega''=0$)$=2.620\pm0.004$ Å and r_0'' (AlCo, $\Omega''=3$)$=2.3833\pm0.0005$ Å. Ionization energies were also measured for all three species, yielding IE(AlV)$=6.01\pm0.10$ eV, IE(AlCr)$=5.96\pm0.04$ eV, and IE(AlCo)$=6.99\pm0.17$ eV. A discussion of these results is presented in the context of previous work on AlCu, AlNi, AlCa, and AlZn.

I. INTRODUCTION

The present study of AlV, AlCr, and AlCo is a continuation of the study of the 3*d* transition metal aluminides recently initiated with the analyses of AlNi[1] and AlCu,[2] and followed by studies of AlCa[3] and AlZn.[4] These studies seek to determine the nature of the interaction between a simple *p*-block group element, Al, and the atoms of the 3*d* transition metal series. Specific chemical bonding considerations to be addressed in this series of investigations are: what is the preferential orientation of the Al 3*p* electron ($3p\sigma$ or $3p\pi$) as the aluminum approaches the transition metal, and what is the role (if any) of $3p\pi_{\mathrm{Al}}$–$3d\pi_{\mathrm{M}}$ bonding in each of the transition metal aluminides.

The initial studies were of the late transition metal aluminides, AlCu[2] and AlNi.[1] These species have ground electronic states which originate from the interaction of a $3d^{m+1}4s^1$ transition metal atom with a $3s^23p^1$ aluminum atom. These electronic configurations are perfectly suited for the formation of a strong σ^2 bond between the 4*s* electron of the transition metal and the 3*p* electron of aluminum in its $p\sigma$ orientation. In the initial studies of AlCu[2] and AlNi[1] bond strengths and bond lengths characterizing this type of interaction were found to be approximately 2.3 eV and 2.3 Å, respectively. These values are similar to those found for late transition metal diatomics formed from atoms with ground state or low-lying electronic configurations of $3d^{m+1}4s^1$, such as Ni_2 ($D_0^0=2.04$ eV; $r_0''=2.15$ Å),[5] NiCu ($D_0^0=2.05$ eV; $r_0''=2.23$ Å),[6] and Cu_2 ($D_0^0=2.03$ eV; $r_e''=2.22$ Å).[7] In contrast, studies of species such as AlCa[3] and AlZn,[4] where the transition metal has a ground configuration of $3d^m4s^2$ and configurations of $3d^{m+1}4s^1$ are energetically or quantum mechanically inaccessible, have shown that the ground state of the AlM molecule derives from a $3p\pi$ approach of the aluminum atom to the filled $4s^2$ subshell. This permits a dative interaction in which electrons from the filled $4s_{\mathrm{M}}$ orbital are partially transferred into the empty $3p\sigma_{\mathrm{Al}}$ orbital, resulting in chemical bonding. Accordingly, ground states of $X\ ^2\Pi_r$ have been found for both AlCa[3] and AlZn.[4] This dative bonding interaction is much weaker than the covalent $3p\sigma_{\mathrm{Al}}$–$4s\sigma_{\mathrm{M}}$ bonding which occurs in AlNi and AlCu, and results in estimated bond strengths below 1 eV and much longer bond lengths of 3.148 and 2.696 Å in AlCa[3] and AlZn,[4] respectively.

As one moves toward the central portion of the 3*d* series, the chemical bonding and expected ground electronic states of the 3*d* transition metal aluminides become generally less obvious. In the case of AlCr, the high stability of the $3d^5(^6S)4s^1$, ^7S ground state of atomic chromium along with its suitability for the formation of a strong $3p\sigma_{\mathrm{Al}}$–$4s\sigma_{\mathrm{Cr}}$ bond make it almost certain that the ground state of the molecule will be a high-spin, $3d^5_{\mathrm{Cr}}(^6S)\sigma^2$, $^6\Sigma^+$ state. In the cases of AlV and AlCo, however, the availability of a number of low-lying excited electronic states in the transition metal atom opens up numerous additional chemical bonding possibilities. Unlike chromium, the ground states of atomic vanadium and cobalt derive from $3d^m4s^2$ configurations and one might expect the bonding in the AlV and AlCo molecules to be analogous to that found in the AlCa and AlZn species, which are characterized by long bond lengths and weak bond strengths. On the other hand, the vanadium and cobalt atoms have rather low-lying $3d^{m+1}4s^1$ configurations which could result in stronger bonds with shorter bond lengths, more akin to our findings for AlCu[2] and AlNi.[1] One of the objectives of the present study is to determine whether the bonding energy gained upon promotion of vanadium or cobalt to the $3d^{m+1}4s^1$ configuration is greater than the energetic cost associated with this promotion. This will be discussed in connection with the experimental results presented below, as will the evidence we have garnered in support of $3p\pi_{\mathrm{Al}}$–$3d\pi_{\mathrm{M}}$ bonding in these species.

Section II provides a brief description of the experimental methods and is followed by the presentation of results in

[a]Kodak Fellow.

 0021-9606/94/101(8)/6487/13/$6.00

Sec. III. In Sec. IV the chemical bonding in these species is discussed based upon the experimental observations, and Sec. V concludes the article with a summary of our most important findings.

II. EXPERIMENT

The pulsed molecular beam, time-of-flight resonant two-photon ionization apparatus used in these studies has been described in detail elsewhere.[8] The creation of the molecular beam results from laser ablation of a metal alloy disk using the second-harmonic radiation of a Q-switched Nd:YAG laser. The ablated metal atoms are entrained in a flow of helium and undergo supersonic expansion to cool the internal degrees of freedom. The success of all spectroscopic studies using this technique is dependent initially upon the ability to create a molecular beam containing the species of interest. In this regard we have found the composition of the metal alloy disk to be a critical factor in producing the molecule.

Details of alloy disk preparation have been presented elsewhere;[9] here we simply note the experimental rule that optimal production of the intermetallic species of interest is obtained using a metal alloy disk that has a composition of the constituent metals that is roughly in inverse proportion to the ratio of the bond strengths of the respective homonuclear dimers. To illustrate, the mole ratio of Al:V employed in the AlV sample disk was chosen to be 3:1 because the bond strength of Al_2 (1.34 ± 0.06 eV)[10] is greatly reduced from that of V_2 (2.753 ± 0.001 eV).[11] This choice of alloy composition discourages the unfavorable exothermic displacement reaction

$$AlV+V\rightarrow Al+V_2 \tag{2.1}$$

and thereby tends to favor production of the mixed metal diatomic, AlV. In contrast, the weaker bond strengths of Cr_2 (1.44 ± 0.05 eV)[12] and Co_2 (0.95 ± 0.26 eV)[13] suggested that 1:1 molar ratios would be suitable for production of AlCr and AlCo. Indeed, an AlCo molecular beam which was adequate for the studies pursued here was created by pulsed laser ablation of a 1:1 mole ratio metal alloy disk. However, all attempts to produce a 1:1 AlCr alloy disk were fruitless because the disk repeatedly shattered upon cooling of the alloy from the melt. To circumvent this difficulty titanium was added to form a 1:1:1 mole ratio alloy. The choice of titanium is advantageous because it not only allows the metals to homogeneously mix, but it also has a high affinity for the oxygen present in the sample, thereby freeing the available AlCr from the complication of oxide formation. In addition, titanium apparently bonds rather weakly to both aluminum and chromium, so that the displacement reactions

$$AlCr+Ti\rightarrow AlTi+Cr \tag{2.2}$$

and

$$AlCr+Ti\rightarrow TiCr+Al \tag{2.3}$$

are not effective in destroying the AlCr that is produced.

The supersonic transition metal aluminide beam is coarsely collimated by a 1 cm skimmer prior to its entrance into the ionization region of a reflectron time-of-flight mass spectrometer. It is in this region in which the resonant two-photon ionization process occurs. The first, excitation photon is supplied by a Nd:YAG-pumped dye laser, which counter-propagates along the molecular beam axis. The ionization laser is fired approximately 10 ns after the excitation laser, and its radiation crosses the molecular beam at right angles. A mass-selected optical spectrum is thus obtained by scanning the Nd:YAG-pumped dye laser while recording the ion signal(s) of interest as a function of dye laser frequency.

A number of different ionization lasers were used to provide the ionization photon in the experiments described in this paper. Low resolution and high resolution scans of the spectra of AlCr and AlV were recorded using an excimer laser operating on KrF (5.00 eV, 248 nm); similar studies on AlCo employed an ArF gas mixture to provide the ionization photon (6.42, 193 nm). The ability to choose the wavelength (and thus the energy) of the ionization photon has allowed this research group to determine (or at least bracket) the ionization energy of a number of metal-containing species.[1–3] In the present study, frequency doubled dye laser radiation generated by passing the output of the dye laser through a servotracked, angle-tuned potassium dihydrogen phosphate (KDP) doubling crystal was utilized as the ionization photon to determine the ionization energy of AlCr. In AlV and AlCo the ionization energies were bracketed by employing an ionization photon created by stimulated Raman scattering of ArF radiation using a high pressure (460 psi) H_2 cell to produce the first Stokes radiation at 210 nm (5.91 eV).

The specific experimental setup used to generate the 5.91 eV (210 nm) radiation consisted of a high pressure cell made from a stainless steel tube 27 in. long and 1 in. in diameter with 1/4-in.-thick walls. Flanges on both ends of the cell hold fused silica (Corning 7940-UV) windows 1 in. thick and 2 in. in diameter, which are rated for a pressure of 2000 psi with a safety factor of 10. The transmission profile of the windows allows transmission of both the fundamental ArF (193 nm) and the Raman shifted Stokes radiation (210 nm), while the anti-Stokes radiation (179 nm) is absorbed. To improve the collimation of the ArF excimer radiation, the laser was fitted with unstable resonator optics. This permitted the beam to be more tightly focused to a point in the center of the Raman cell using a 70 cm focal length lens (measured at 500 nm). The laser was then operated at energies of 50–100 mJ/pulse and the output radiation was collimated with a second lens of the same focal length. The Stokes shifted radiation was separated from the fundamental radiation using a dielectric mirror (ARC 193FR-45-2D-FL) which at 45° incidence reflects 95% of the 193 nm fundamental radiation and transmits 70% of the 210 nm radiation. The remaining 193 nm radiation that was transmitted could be successfully absorbed by a 1 cm KBr window which transmitted roughly 30% of the 210 nm radiation. Salt windows made of NaCl were similarly effective in completely absorbing the residual ArF radiation while still passing sufficient quantities of the 210 nm radiation for photoionization.

Although no quantitative measurements have been made to determine the efficiency of Stokes light generation, it was obvious that the conversion efficiency was far less than the value of 50% reported by Loree *et al.* for H_2 Raman shifting of KrF.[14] We estimate a conversion efficiency of 10%–20%

using 500 psi H_2, providing ionization laser energies of approximately 5 mJ/pulse. This was adequate for the interrogation of AlV and AlCo in the molecular beam.

The vibronic spectra of AlV, AlCr, and AlCo were congested at even moderate excitation energies, thus necessitating the use of Raman shifted dye laser radiation in order to locate discrete transitions in the infrared energy region of the spectrum. A similar Raman shifting apparatus, of smaller dimensions than that described above, was utilized to shift the fundamental output of the dye laser. As described by Clouthier and Karolczak,[15] the H_2 Raman shifting process occurs exclusively on the $Q(1)$ line, and at 500 psi this results in a Raman shift of 4155.162 cm^{-1}. Thus it became possible to extend the range of the excitation photon down to about 8800 cm^{-1} employing this experimental arrangement.

High resolution (0.04 cm^{-1}) rotationally resolved spectra were recorded by the insertion of an air-spaced intracavity étalon into the dye laser, which was pressure scanned from 0 to 1 atm with Freon 12 (CCl_2F_2, DuPont). Most of the bands rotationally resolved in this study were at frequencies which required the use of the H_2 Raman shifter as described above. In turn, either the fundamental output of the dye laser or the anti-Stokes radiation generated in these experiments was used to simultaneously record an I_2 transmission spectrum for calibration purposes in comparison with the I_2 atlas of Gerstenkorn and Luc.[16] The calibration of the rotationally resolved data was completed by applying a final correction for the Doppler shift experienced by the molecules as they traveled toward the radiation source at the beam velocity of helium (1.77×10^5 cm/s), amounting to less than 0.08 cm^{-1}.

Excited state lifetimes were measured by the time-delayed resonant two-photon ionization method in which the delay between the excitation and ionization lasers is varied and the ion signal is recorded as a function of this delay. The resulting data set was fitted to an exponential decay model using a nonlinear least-squares algorithm, which allowed the $1/e$ lifetime of the excited electronic states to be extracted.[17]

III. RESULTS

A. Bond strengths of AlV, AlCr, and AlCo

In a number of transition metal-containing molecules studied in this group abrupt predissociation thresholds have been observed in a forest of vibronic transitions and it has been argued that these correspond to the thermochemical bond strength of the molecule.[1,9,11,18,19] It is believed that in most of these species the density of electronic states near the dissociation limit is so great that a breakdown of the Born–Oppenheimer approximation occurs and predissociation mechanisms set in as soon as the energy of the ground state separated atoms is surpassed. Spectroscopically this breakdown is observed as an abrupt threshold above which no optical transitions are observed due to rapid dissociation on a subnanosecond time scale. Thus, the excited molecules predissociate before they can be ionized, making the transition undetectable by the resonant two-photon ionization technique. Several rules regarding this phenomenon have been summarized elsewhere,[19] but generally predissociation at the thermochemical threshold occurs because of the extremely large density of states in these species, combined with nonadiabatic couplings between the adiabatic potential curves. In cases where the density of electronic states is not so severe, however, it appears that predissociation may not set in until a separated atom limit is reached which generates repulsive potential energy curves.

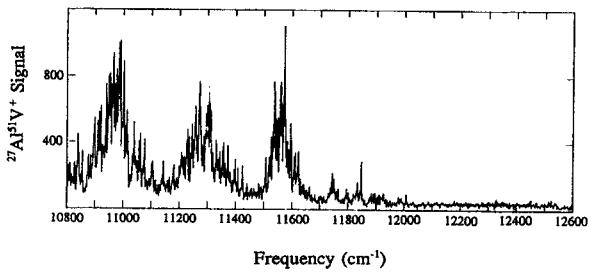

FIG. 1. Predissociation threshold in diatomic $^{27}Al^{51}V$ obtained by resonant two-photon ionization spectroscopy using rhodamine 640 and 640/DCM 1:1 mix laser dyes, Raman shifted in high pressure H_2, for excitation and KrF excimer radiation for photoionization. In addition to the predissociation threshold at 12 007 cm^{-1}, a distinct pattern of clumps of intensity in this dense vibronic spectrum is observed.

The density of electronic states in a particular molecule can be estimated very simply by a calculation of the number of Hund's case (c) potential energy curves arising from each separated atom limit. In combining two atoms in spin–orbit levels with total angular momentum J_A and J_B, the resultant number of distinct relativistic adiabatic [case (c)] potential energy curves equals $[(2J_A+1)(2J_B+1)]/2$ if J_A+J_B is half-integer, and $(2J_<+1)(J_>+1)$ distinct curves if J_A+J_B is an integer. Summation of the number of curves which result from all separated atom limits below a specified energy, E, yields an integrated density of electronic states at the separated atom limit, $N(E)$. As has been shown for AlNi,[1] the opening of the $3d$ subshell of the transition metal results in a large number of possible angular momentum couplings, generating many distinct potential energy surfaces (141 within 15 000 cm^{-1} of the Al+Ni ground state separated atom limit). In AlCr a similar density of states is generated [$N(15\,000\ cm^{-1})=111$] while AlCo has more than twice this density of states, $N(15\,000\ cm^{-1})=284$, and AlV has the greatest density of states of all of the $3d$ transition metal aluminides with $N(15\,000\ cm^{-1})=454$. As might be expected, all three of these molecules, display abrupt predissociation thresholds.

The predissociation threshold in diatomic AlV at 12 007 cm^{-1} is displayed in Fig. 1. The observation of a predissociation threshold in the near infrared is unprecedented in work from this group. Previously observed predissociation thresholds have been found at much higher frequencies (above 16 000 cm^{-1}), and it has been found that the spectra tend to thin out toward lower excitation energies.[1,9,11] In contrast, AlV exhibits a very dense vibronic spectrum at energies as low as 10 600 cm^{-1}. As displayed in Fig. 1, this spectrum can be characterized as having "clumps" of intense transitions at frequency intervals of approximately 300 cm^{-1}. We surmise that this phenomenon may occur because an electronic state with high oscillator strength couples with nearby

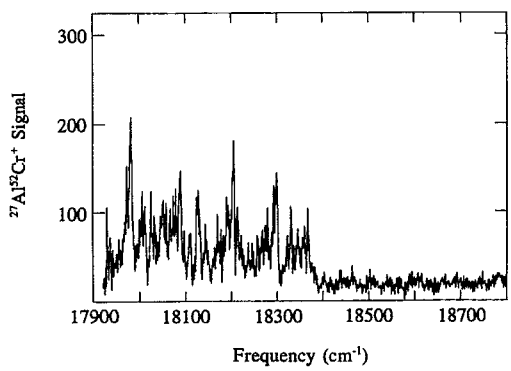

FIG. 2. Low resolution vibronic spectrum of $^{27}Al^{62}Cr$ collected utilizing coumarin 540A laser dye in conjunction with KrF laser radiation in the two-photon process. The dense vibronic spectrum terminates abruptly at 18 377 cm^{-1}, allowing the AlCr bond strength to be determined as $D_0^0(AlCr)=2.272\pm0.009$ eV.

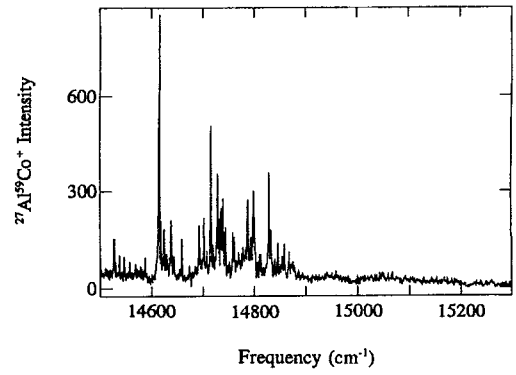

FIG. 3. Low resolution resonant two-photon ionization spectrum of $^{27}Al^{59}Co$ recorded employing DCM/LDS 698 1:1 laser dye mix for excitation and Raman shifted ArF radiation for photoionization. The predissociation threshold in AlCo observed at 14 876 cm^{-1} occurs in a relatively sparse energy region composed of discrete vibronic bands in contrast to the absorption quasicontinuum that is commonly observed in open d-subshell transition metal-containing species.

states, allowing them to gain oscillator strength in the process. The clumps of intensity in the spectrum, which are reproducible and are not related to the variation in laser fluence as one scans across a dye curve, then probably represent a series of vibrational levels of the state or states with high oscillator strength, and the widths of these clumps are related to the matrix elements coupling the "bright" state with the underlying "dark" states.

At energies below 11 600 cm^{-1} the vibronic transitions in AlV are quite intense (as shown in Fig. 1), while at energies between 11 600 cm^{-1} and the predissociation threshold (12 007 cm^{-1}) the transitions are much weaker although still highly reproducible. A possible reason for this decrease in intensity at higher energies could be that the excited states accessed in the 11 600–12 007 cm^{-1} range do predissociate, but on a time scale that is competitive with ionization. To test this possibility lifetimes of the excited states of the bands at 11 848 and 12 007 cm^{-1} were measured by the time-delayed R2PI technique, yielding values of 11 and 16 μs, respectively. It is apparent that predissociation is not competitive with photoionization in these bands; rather, it appears that the transitions in the 11 600–12 007 cm^{-1} energy region simply have a reduced oscillator strength as compared to the lower energy bands. Based on the observed predissociation threshold at 12 007 cm^{-1}, a bond strength of $D_0^0(AlV)=12007\pm80$ cm^{-1} (1.489±0.010 eV) is assigned, where a generous error limit of 80 cm^{-1} is included to account for the possibility of weak features to the blue of 12 007 cm^{-1} which are not predissociated.

A weaker, but nevertheless reproducible, predissociation threshold was observed in AlCr at 18 377 cm^{-1}, as displayed in Fig. 2. The band at 18 377 cm^{-1} was investigated under high resolution (0.04 cm^{-1}) in order to calibrate the predissociation threshold by simultaneously monitoring the precisely known transmission spectrum of I_2.[16] As will be discussed further in Sec. III C the ground state of AlCr is almost certainly the $3d_{Cr}^5(^6S)3s_{Al}^2\sigma^2$, $^6\Sigma^+$ state which has $\Omega''=1/2$, 3/2, and 5/2 levels. The higher lying, presumably repulsive $3d_{Cr}^5(^6S)3s_{Al}^2\sigma^1\sigma^{*1}$, $^8\Sigma^+$ state, which generates repulsive substates with $\Omega=1/2$, 3/2, 5/2, and 7/2, and which correlates to ground state atoms provides a convenient means for the $\Omega=1/2$, 3/2, 5/2, and 7/2 states (which may be accessed by optical excitation from the different sublevels of the $X\ ^6\Sigma^+$ ground state) to predissociate while preserving their value of Ω. However, all of the Ω sublevels arising from the repulsive $^8\Sigma^+$ state adiabatically correlate to the spin–orbit excited separated atom limit of Al $(3s^23p^1,{}^2P_{3/2}^0)$+Cr $(3d^54s^1,{}^7S_3)$. On this basis it seems reasonable to correct the experimentally measured predissociation threshold, 18 377±15 cm^{-1}, by the spin–orbit energy of the aluminum $^2P_{3/2}^0$ state (112.04 cm^{-1})[20] and to increase the error limit to include the possibility of predissociation at the ground separated atom limit of Al $(3s^23p^1,{}^2P_{1/2}^0)$+Cr $(3d^54s^1,{}^7S_3)$. Accordingly, the dissociation energy of AlCr is determined as $D_0^0(AlCr)=18321\pm70$ cm^{-1}=2.272±0.009 eV, where the error limit reflects the uncertainty as to whether predissociation occurs to ground state atoms or to a spin–orbit excited aluminum atom.

In contrast to the examples of AlV and AlCr, the predissociation threshold displayed in Fig. 3 for AlCo exhibits a somewhat lower density of vibronic transitions than are found in the former molecules. Nevertheless, it is apparent that there is a predissociation threshold, because no spectroscopic transitions are observed to the blue of 14 900 cm^{-1}. In this example the predissociation threshold was determined by selecting the highest energy reproducible feature, the transition at 14 876 cm^{-1}, and attaching an uncertainty of ±15 cm^{-1}, allowing a final determination of $D_0^0(AlCo)=1.844\pm0.002$ eV to be made. It should be noted that AlCo is a molecule which exhibits a predissociation threshold although no repulsive curves arise from its ground state separated atom limit. A similar situation was observed recently in Co_2^+[19] in which an onset of abrupt predissociation occurred despite the absence of repulsive curves at the lowest separated atom limit. In that former study it was suggested that if the density of states of a molecule is great enough, weaker predissociation processes that do not require curve crossings with repulsive states can dominate merely by

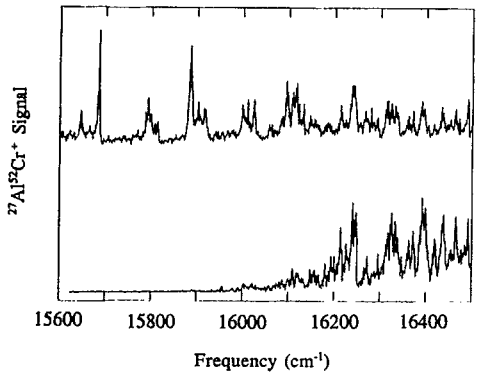

FIG. 4. Determination of the ionization threshold of AlCr. In the lower spectrum frequency-doubled rhodamine 640/DCM 1:1 dye light is employed as the ionization photon and the R2PI scheme. The upper scan is recorded using fixed frequency KrF excimer radiation (5.0 eV, 248 nm) for photoionization. The last band definitely observed using the frequency-doubled dye light occurs at 16 111 cm^{-1}, allowing the ionization energy of AlCr to be determined as 5.96±0.04 eV, including a correction for the field ionization effect.

strength of numbers. It appears that this phenomenon is also operating in AlCo.

B. Ionization energies of AlV, AlCr, and AlCo

In the resonant two-photon ionization scheme, the second, ionization photon is selected such that it is energetically capable of photoionizing the excited state which is produced following the absorption of the first, excitation photon. By utilizing less energetic ionization photons in a systematic manner it is often possible to determine the ionization energy of a given neutral species by determining the minimum energy required for production of the cation.

The low resolution spectrum of AlCr was recorded using KrF laser radiation (5.00 eV, 248 nm) for photoionization. A portion of the resulting spectrum is displayed in the upper trace of Fig. 4. The lower trace, in contrast, was collected using the second harmonic of the dye laser radiation for photoionization. At the high frequency end of Fig. 4, the major features present in the dye radiation+KrF radiation two-photon process are also present in the dye+doubled dye two-photon experiment. As one scans to lower frequencies using the dye+doubled dye process, however, the signal weakens and eventually disappears because the sum of the two photon energies is no longer sufficient to ionize the AlCr molecule. The ionization threshold displayed in Fig. 4 is not extremely sharp and this may be due to either vibrationally excited ($v''=1$) molecules in the molecular beam or to Frank–Condon difficulties in the ionization step. Nevertheless, from a comparison of the two spectra it is possible to assign the ionization energy of AlCr as 5.96±0.04 eV. This determination was made by first averaging the frequencies of the band at 16 111 cm^{-1} (which is ionized by the doubled dye photon, as demonstrated in the lower panel) and the band at 15 886 cm^{-1} (which is not ionized by frequency doubled dye laser radiation and is thus absent in the lower panel). This value is then multiplied by three to account for the $\omega+2\omega$ ionization process, and finally corrected for the expected field ionization shift due to the electric field of the time-of-flight electrodes, amounting to ≈0.01 eV. The uncertainty is accordingly calculated as three times the energy difference between the aforementioned bands.

The ionization energies of diatomic AlV and AlCo were also measured by the comparison of spectra generated using different excimer-generated ionization photon energies. The majority of the spectroscopic work performed on AlV was accomplished utilizing KrF laser radiation for photoionization. The vibronic spectrum of AlV was scanned from far above the predissociation threshold down to nearly 8800 cm^{-1}. The observation of the lowest energy vibronic transition at 8881 cm^{-1} sets an upper limit on the ionization energy of AlV of IE(AlV)<6.109±0.003 eV, where this value is merely a summation of the energies of the excitation and ionization photons (and includes a correction for the field ionization effect). The uncertainty reported reflects the range of photon energies emitted by the KrF laser according to the manufacturer. This upper limit indicates that ArF radiation (6.42 eV, 194 nm) is capable of one-photon ionizing diatomic AlV. However, Raman shifting the ArF radiation in high pressure H_2 results in Stokes radiation at 210 nm (5.905 ±0.004 eV), which could still lie below the ionization energy of AlV. An experiment was therefore attempted using Raman shifted ArF radiation for photoionization. If this wavelength were capable of one-photon ionizing diatomic AlV, no resonant enhancement would be observed and this would reduce the upper limit on the ionization energy to 5.91 eV. On the other hand, if resonant transitions could still be observed using 210 nm radiation for photoionization a lower limit would be placed on the ionization energy of 5.91 eV. Low resolution scans performed in this manner produced spectra that looked similar to those collected using KrF radiation for photoionization, although with a reduced signal-to-noise ratio. In addition, with the dye laser tuned to the band at 11 570 cm^{-1}, mass spectra were recorded both with and without dye laser radiation entering the spectroscopy chamber. When the 11 570 cm^{-1} radiation was allowed to enter the chamber a fivefold resonant enhancement of the $^{27}Al^{51}V$ mass peak resulted. This experiment therefore bracketed the ionization energy of AlV, again including field ionization corrections, between 5.915±0.004 eV (where the uncertainty now reflects the range of photon energies emitted by the ArF laser according to the manufacturer) and 6.109 ±0.003 eV, yielding an average value of IE(AlV)=6.01 ±0.10 eV, where the uncertainty now reflects the overall error in the averaged value.

ArF laser radiation was employed for photoionization in the resonant two-photon ionization spectroscopy of AlCo. The spectral region investigated in low resolution ranged from 18 450 cm^{-1} (again well above the dissociation energy of this molecule) down to approximately 9950 cm^{-1}. The observation of a band at 9981 cm^{-1} initially set an upper limit for the ionization energy of AlCo as IE(AlCo)<7.64 eV (again given by the summation of the excitation and the ionization photon energies). Furthermore, the ability to observe resonant enhancement using ArF radiation immediately provided a lower limit on the ionization energy of 6.42 eV <IE(AlCo). Next, Raman shifted ArF radiation (210 nm)

was employed for photoionization, and the band at 9981 cm^{-1} was still resonantly enhanced, placing a new upper limit on the ionization energy of IE(AlCo)<7.153±0.005 eV. This limit includes a shift for the field ionization effect and the uncertainty again reflects the range in photon energies emitted by the ArF laser according to the manufacturer. Finally, KrF laser radiation (5.00 eV, 248 nm) was employed for photoionization; however, even the highest energy band observed using ArF (at 14 613 cm^{-1}) was not resonantly enhanced. In the absence of an accidental resonance with the 5.00 eV KrF radiation this provides a lower limit of IE(AlCo)>6.8194±0.0031 eV. From these upper and lower limits IE(AlCo)=6.99±0.17 eV is determined, again including a field ionization correction which amounted to approximately 0.011 eV.

C. Bond strengths of AlV$^+$, AlCr$^+$, and AlCo$^+$

The experimental determination of the neutral bond strengths and ionization energies of AlV, AlCr, and AlCo allows the bond strengths of the respective cations to be calculated by referencing the atomic ionization energies of Al (5.985 77 eV)[21] and V, Cr, and Co, respectively,[22–24] followed by completion of the thermodynamic cycles:

$$D_0^0(Al^+-M)=D_0^0(Al-M)+IE(Al)-IE(AlM) \quad (3.1)$$

and

$$D_0^0(Al-M^+)=D_0^0(Al-M)+IE(M)-IE(AlM), \quad (3.2)$$

where M is the appropriate transition metal. In this manner estimated cationic bond strengths of $D_0^0(Al^+-V)$ =1.48±0.10 eV, $D_0^0(Al-V^+)$=2.24±0.10 eV, $D_0^0(Al^+-Cr)$ =2.30±0.05 eV, $D_0^0(Al-Cr^+)$=3.08±0.05 eV, $D_0^0(Al^+-Co)$ =0.84±0.17 eV, and $D_0^0(Al-Co^+)$=2.72±0.17 eV are deduced.

D. Rotationally resolved studies of AlV, AlCr, and AlCo

As demonstrated by Figs. 1–3, the spectra of the open $3d$ subshell transition metal aluminides are very congested in the region close to the predissociation threshold and it is generally impossible to discern vibrational progressions in any single excited electronic state. Indeed, in this region of the spectrum it would probably be difficult if not impossible to find an excited vibronic level which is free from perturbations from nearby states. In general, however, as one scans the excitation frequency to lower energies, the forest of excited states thins out sufficiently to allow isolated, discrete bands to be located. Even at energies as low as 9000 cm^{-1}, however, it would be a monumental and probably pointless task to attempt to identify and characterize the individual excited electronic states in either AlV or AlCo. Although rotationally resolved scans of bands in this energy region would do little to elucidate the electronic structure of the excited states, such high resolution analyses can yield important information relevant to the ground state chemical bonding characteristics of the molecule.

Initial attempts to rotationally resolve diatomic AlCr were fruitless, and not much effort was expended on this molecule. The high resolution spectra consisted of numerous lines, none of which were recognizable as forming an interpretable R, Q, and P branch structure. As mentioned above, the ground state of AlCr almost certainly derives from a $3p\sigma-4s\sigma$ bonding interaction between the $3s^2 3p^1$, $^2P^0$ aluminum and $3d^5(^6S)4s^1$, ^7S chromium atoms, resulting in a $3s^2_{Al}3d^5_{Cr}(^6S)\sigma^2$, $^6\Sigma^+$ ground state. In such a state the second-order spin–orbit splitting into Ω=1/2, 3/2, and 5/2 levels would be expected to be small, causing the state to belong to either Hund's case (b) or to a case intermediate between case (a) and case (b). This could easily lead to the complex rotational structure that was observed. In any event no serious attempt was made to analyze the rotationally resolved spectra.

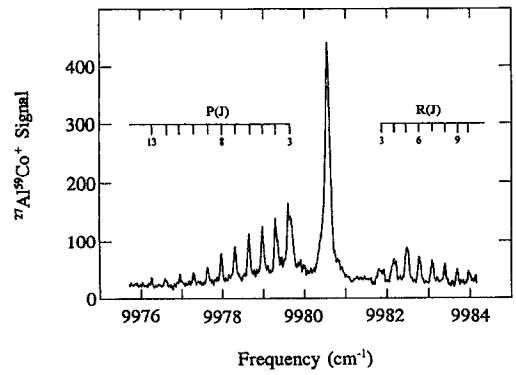

FIG. 5. Rotationally resolved scan of the 9981 cm^{-1} band of $^{27}Al^{59}Co$, recorded using LDS 698 dye laser radiation, Raman shifted in high pressure H_2, in conjunction with ArF radiation (6.42 eV, 193 nm) for photoionization. The band is fit as a $\Omega'=2\leftarrow\Omega''=3$ transition and the absence of band heads suggests very little change in bond length upon electronic excitation.

High resolution scans over individual vibronic bands of AlCo were considerably more informative. Four bands were successfully rotationally resolved, including the 9981 cm^{-1} band of $^{27}Al^{59}Co$ displayed in Fig. 5. This band exhibits an intense Q branch and a P branch with greater intensity than the R branch, as is characteristic of a perpendicular transition with $\Delta\Omega=-1$. The gaps between the Q branch and the R and P branches demonstrate that certain low-J rotational lines are absent, indicating that $\Omega''>1$. Of the possible $\Omega'\leftarrow\Omega''$ transition assignments of $1\leftarrow2$, $2\leftarrow3$, $3\leftarrow4$, etc., all of the lines were accounted for and the best fit was obtained for an $\Omega'=2\leftarrow\Omega''=3$ transition, which was fitted to the standard formula

$$\nu=\nu_0+B'J'(J'+1)-B''J''(J''+1). \quad (3.3)$$

The absolute line positions, found in Table I, were obtained following calibration with the I_2 atlas of Gerstenkorn and Luc[16] and adjustment for the Doppler shift as discussed in Sec. II. The absence of a bandhead in either the P or the R branch indicates little change in the bond length upon electronic excitation. This was confirmed by the fit of the rotational lines, which provided ground and excited state bond lengths of r_0'' = 2.3831 ± 0.0006 Å and r_0' = 2.3911 ± 0.0006 Å, respectively.

It is also apparent in the spectrum displayed in Fig. 5 that the first rotational lines of the R and P branches are

TABLE I. Rotationally resolved and analyzed bands of $^{27}Al^{59}Co$.[a]

Line	9981 cm^{-1} band $\Omega'=2\leftarrow\Omega''=3$	11 439 cm^{-1} band $\Omega'=4\leftarrow\Omega''=3$	12 206 cm^{-1} bands $\Omega'=4\leftarrow\Omega''=3$	12 206 cm^{-1} bands $\Omega'=4\leftarrow\Omega''=3$
$P(13)$	9976.257 (0)			
$P(12)$	9976.601(−2)			
$P(11)$	9976.952 (5)			
$P(10)$	9977.288(−2)		12 203.239 (36)	
$P(9)$	9977.627(−2)		12 203.558 (13)	
$P(8)$	9977.967 (0)		12 203.874(−10)	
$P(7)$	9978.301(−2)		12 204.199(−22)	
$P(6)$	9978.641 (4)		12 204.521(−34)	
$P(5)$	9978.973 (5)			
$P(4)$	9979.288(−9)			
$P(3)$	9979.630 (5)			
$Q(13)$		11 436.891 (0)		
$Q(12)$		11 437.150 (9)		
$Q(11)$		11 437.367 (−5)		
$Q(10)$		11 437.575 (−9)		
$Q(9)$		11 437.771 (−5)		
$Q(8)$		11 437.942 (−7)		12 204.798 (15)
$Q(7)$		11 438.083(−20)		12 205.076 (−2)
$Q(6)$				12 205.310(−26)
$Q(5)$				12 205.551 (−6)
$Q(4)$		11 438.499 (49)		12 205.760 (18)
$R(3)$	9981.850(−5)	11 439.739 (10)		12 207.030 (8)
$R(4)$	9982.163(−2)	11 439.954 (1)	12 208.033(−30)	12 207.154 (−3)
$R(5)$	9982.479 (6)	11 440.149 (−8)	12 208.361 (−6)	12 207.248 (−8)
$R(6)$	9982.771(−8)	11 440.321(−21)	12 208.683 (15)	12 207.322 (4)
$R(7)$	9983.087 (4)	11 440.509 (1)	12 208.993 (27)	
$R(8)$	9983.389 (5)	11 440.640(−14)	12 209.293 (31)	
$R(9)$	9983.688 (5)	11 440.776 (−6)	12 209.581 (25)	
$R(10)$	9983.974(−7)	11 440.892 (2)	12 209.863 (17)	
$R(11)$		11 440.992 (13)	12 210.120(−15)	
$R(12)$			12 210.372(−49)	
$R(13)$		11 441.109 (10)		

[a]All line positions are given in wave numbers (cm^{-1}), calibrated using the absorption spectrum of I_2 as described in the text. A correction was also applied to account for the Doppler shift experienced by the AlCo molecules as they traveled toward the radiation source at the beam velocity of helium (1.77×10^5 cm/s). Residuals in the least-squares fit of the line positions to $\nu=\nu_0+B'J'(J'+1)-B''J''(J''+1)$ are given in units of 0.001 cm^{-1} following each entry in parentheses. Fitted parameters for the bands (with 1σ error limits) are: 9981 cm^{-1} band: ν_0=9980.5932 (22), B_0'' = 0.160 38 (7), B'=0.159 32 (8); 11 439 cm^{-1} band: ν_0=11 438.6424 (83), B_0'' = 0.159 90 (43), B'=0.150 28 (41); 12 206 cm^{-1} bands: ν_0=12 206.5066 (177), B_0'' = 0.159 46 (57), B'=0.158 18 (48); ν_0=12 206.1104 (146), B_0'' = 0.159 98 (92), B'=0.141 54 (98).

broadened as compared to the higher J lines. This is almost certainly due to unresolved hyperfine splittings which could arise from the interaction of the electron spin with either the nuclear spin of ^{27}Al ($I=5/2$) or of ^{59}Co ($I=7/2$). As is discussed in Sec. IV B below, we believe the hyperfine splittings originate primarily from ^{59}Co, although this is not proven. The widths of the hyperfine-broadened rotational lines appear to be roughly inversely proportional to J, as is consistent with case (a_β) coupling, where the hyperfine energy is given by[25]

$$E_{\rm hf}=[a\Lambda+(b+c)\Sigma]\frac{\Omega}{J(J+1)}\times\left(\frac{F(F+1)-J(J+1)-I(I+1)}{2}\right). \tag{3.4}$$

In this expression, the a, b, and c parameters reflect expectation values of the unpaired electron at or near the magnetically active nucleus, as given by the formulas

$$a=g_e g_I \mu_0 \mu_n \langle r^{-3}\rangle, \tag{3.5}$$

$$b\approx g_e g_I \mu_0 \mu_n \{(8\pi/3)\psi^2(0)-\langle(3\cos^2\chi-1)/2r^3\rangle\}, \tag{3.6}$$

and

$$c\approx 3 g_e g_I \mu_0 \mu_n \langle(3\cos^2\chi-1)/2r^3\rangle, \tag{3.7}$$

where g_e and g_I are the electronic and nuclear g factors, μ_0 and μ_n are the Bohr and the nuclear magneton, respectively, $\psi^2(0)$ reflects the probability that the unpaired electron will be located at the magnetic nucleus, r is the distance of the electron from the magnetic nucleus, and χ is the angle between the nucleus-to-electron vector and the internuclear axis.[26] Brackets indicate expectation values.

In addition to the observation that the low J lines are preferentially broadened, the widths of P and R branch lines terminating on the same upper state [such as $R(3)$ and $P(5)$] are quite different, with $P(5)$ being considerably more nar-

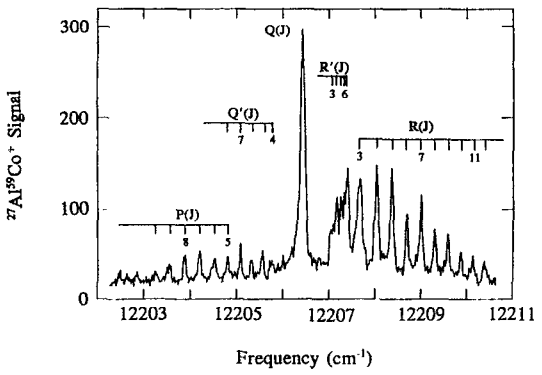

FIG. 6. Two rotationally resolved $\Omega'=4\leftarrow\Omega''=3$ bands of AlCo collected using Raman shifted rhodamine 640/DCM 1:1 mix for excitation and ArF excimer laser radiation for photoionization. As described in greater detail in the text, the two bands are believed to correspond to transitions excited by the first and second Stokes radiation generated by the H_2 Raman shifting process.

row than $R(3)$. On the other hand, the widths of P and R branch lines originating from the same lower state [such as $R(3)$ and $P(3)$] are comparable. This indicates that the hyperfine splitting is larger in the lower state than in the upper state. In most molecules exhibiting large hyperfine effects the dominant term is the Fermi contact interaction, which is represented by the term in b involving $\psi^2(0)$.[25] This term only makes a significant contribution when unpaired electron density lies in a σ orbital, which can take on some atomic s character and thereby result in finite values of $\psi^2(0)$. To illustrate the possible relative magnitudes of the hyperfine parameters a, b, and c, we note that the Fermi contact portion of the b parameter would give $b=5947$ MHz (0.198 cm^{-1}) for a single electron in a pure $4s$ orbital on cobalt, while $b=3911$ MHz (0.130 cm^{-1}) would result for a single electron in a pure $3s$ orbital on aluminum.[27] In contrast to these rather large values of b, the maximum possible values of a and c may be estimated from the atomic expectation value of $\langle r^{-3}\rangle$, providing values of $g_e g_L \mu_0 \mu_n \langle r^{-3}\rangle = 845$ MHz (0.028 cm^{-1}) and 208 MHz (0.007 cm^{-1}) for a cobalt $3d$ electron and an aluminum $3p$ electron, respectively.[27] Assuming that the hyperfine splitting arises entirely from the lower state, and anticipating the identification of this as the $X\ ^3\Delta_{3,i}$ ground state, the width of the $R(3)$ feature leads to a value of $(2a+b+c)\approx 0.04$ cm^{-1}. This large value suggests strongly that the ground electronic state of AlCo has an unpaired electron in a σ orbital, as will be further discussed in Sec. IV B below.

Another high resolution scan of AlCo is displayed in Fig. 6. When these data were originally collected, it was believed that a single vibronic band was being investigated. It soon became evident, however, that the gap between the Q and R branches was not as large as in the 9981 cm^{-1} band, suggesting a lower value of Ω'' in the band displayed in Fig. 6. Even employing a reduced value of Ω'', however, attempts to fit the observed structure in the band met with no success. Finally, the possibility that two overlapping bands are present in Fig. 6 was considered, and the bands were both eventually fit as $\Omega'=4\leftarrow\Omega''=3$ transitions, yielding ground state rotational constants that were consistent with the B'' value determined from analysis of the 9981 cm^{-1} band.

The more intense lines which fan out on either side of the strong Q branch are labeled by the $P(J)$ and $R(J)$ labels in Fig. 6, and these belong to a single band. In this band, the greater intensity of the R branch as compared to the P branch indicates a $\Delta\Omega=+1$ type of transition and the absence of a bandhead in either branch suggests again that the ground and excited state bond lengths are similar. Labels of $R'(J)$ and $Q'(J)$ are used to designate the weaker rotational lines associated with the second band in Fig. 6. In this feature the R branch is more intense than the Q branch, while the P branch is too weak to be observed, again consistent with a $\Delta\Omega=+1$ type of transition. Further, this second band exhibits a severe bandhead in the R branch signifying a bond lengthening upon electronic excitation. Line positions for both bands can be found in Table I.

The observation of two $\Omega'=4\leftarrow\Omega''=3$ transitions at the same energy is quite surprising, particularly since they appear to originate from the same lower state. This implies that the energy of the upper state is very nearly the same for the two bands, and one would ordinarily expect homogeneous perturbations to couple the two $\Omega'=4$ states, causing significant energy shifts, and errors in the fit of the rotational line positions to Eq. (3.3). The errors in the line positions fit to Eq. (3.3) for the more intense band do indeed suggest a definite perturbation in the upper state. The lines which terminate on the same upper state J' level have errors of approximately the same magnitude and in the same sense, indicating that the upper rotational level has been shifted from its unperturbed energy. For example, the $R(3)$ and $P(5)$ pair of lines are displaced 0.060 cm^{-1} to the red of their expected positions, while the $R(8)$ and $P(10)$ lines have been shifted approximately 0.038 cm^{-1} to the blue of their expected energies. The errors associated with the $R(3)$ and $P(5)$ lines were by far the greatest and as a result this pair of lines was omitted from the final rotational fit in order to obtain the best estimate of the ground state rotational constant for $^{27}Al^{59}Co$. If indeed the two excited states displayed here are perturbing one another one would expect the line positions of the weaker band to follow a similar pattern. However, the rotational structure of this band is well modeled with the standard formula [Eq. (3.3)], demonstrating that it cannot be the perturber responsible for the anomalies in the fit of the more intense band.

The apparent lack of perturbation between these two $\Omega'=4$ upper states would be explained if they were not really at the same energy. This is possible, because when the experiments were carried out the laser radiation near 12 206 cm^{-1} was generated by Raman shifting fundamental dye laser radiation near 16 361 cm^{-1} in high pressure hydrogen. The fundamental radiation and the anti-Stokes radiation then lay above the AlCo predissociation threshold, and could not be responsible for any observed transitions. However, it is possible that a second transition was excited by the second Stokes radiation near 8051 cm^{-1}, and this could be responsible for the second set of features in the spectrum. At the time the spectrum was collected this possibility seemed remote, so no attempts were made to prevent the second Stokes

TABLE II. Rotationally resolved and analyzed bands of $^{27}Al^{51}V$.[a]

Line	9074 cm^{-1} band $\Omega'=2\leftarrow\Omega''=1$	9081 cm^{-1} band $\Omega'=1\leftarrow\Omega''=0$	10 078 cm^{-1} band $\Omega'=1\leftarrow\Omega''=0$
$P(8)$	9070.682(−18)		
$P(7)$	9071.251 (9)		
$P(6)$	9071.742 (−4)	9079.190 (−7)[b]	
$P(5)$	9072.220 (8)	9079.687 (1)[b]	10 076.253(−15)
$P(4)$	9072.626(−14)	9080.150 (17)[b]	10 076.720(−11)
$P(3)$		9080.540 (3)[b]	10 077.162 (15)
$P(2)$	Missing	9080.896 (−4)[b]	10 077.536 (18)
$Q(7)$	9072.916 (13)		10 076.839 (5)
$Q(6)$	9073.184 (14)		10 077.162 (6)
$Q(5)$	9073.407 (9)		10 077.438 (6)
$Q(4)$	9073.590 (1)		10 077.659 (−3)
$Q(3)$	9073.746 (5)	9080.896 (15)[b]	10 077.843 (−2)
$Q(2)$	9073.857 (1)	9081.154(−36)[b]	10 077.979 (−4)
$Q(1)$	Missing	9081.410 (15)[b]	10 078.070 (−5)
$R(0)$	Missing	9081.695(−39)[b]	10 078.360 (6)
$R(1)$	9074.412 (6)	9081.939 (11)[b]	10 078.530(−11)
$R(2)$	9074.559 (−8)	9082.097 (17)[b]	10 078.667(−14)
$R(3)$	9074.695 (5)	9082.207 (18)[b]	10 078.776 (0)
$R(4)$	9074.764(−11)	9082.255 (−1)[b]	10 078.839 (14)
$R(5)$	9074.809(−13)		10 078.839 (11)
$R(6)$		9082.255 (−9)[b]	10 078.776 (−8)
$R(7)$			10 078.688 (−7)

[a]All line positions are given in wave numbers (cm^{-1}), calibrated using the absorption spectrum of I_2 as described in the text. A correction was also applied to account for the Doppler shift experienced by the AlV molecules as they traveled toward the radiation source at the beam velocity of helium (1.77×10^5 cm/s). Residuals in the least-squares fit of the line positions to $\nu=\nu_0+B'J'(J'+1)\mp\frac{1}{2}q'J'(J'+1)-B''J''(J''+1)$ are given in units of 0.001 cm^{-1} following each entry in parentheses. The Λ-doubling parameter, q', was only required for the 9081 cm^{-1} band. Fitted parameters are as follows. 9074 cm^{-1} band: ν_0=9073.9700 (55), $B_0''(\Omega=1)$ = 0.137 68 (34), B'=0.118 62 (42); 9081 cm^{-1} band: ν_0=9081.4984 (93), $B_0''(\Omega=0)$ = 0.139 07 (82), B'=0.102 79 (118), q'=−0.030 38 (172); 10 078 cm^{-1} band: ν_0=10 078.1214 (39); $B_0''(\Omega=0)$ = 0.139 34 (44); B'=0.116 34 (37).

[b]For the 9081 cm^{-1} band the proper branch labels are $R_a(J)$, $Q_{ba}(J)$, and $P_a(J)$.

radiation from entering the apparatus. Studies employing a short pass filter would be required to verify this hypothesis.

One last $\Omega'=4\leftarrow\Omega''=3$ band at 11 439 cm^{-1} was also rotationally resolved and the rotational line positions are given in Table I. A weighted least squares determination of the ground state rotational constant based on the lower state rotational constants of all four rotationally resolved bands was performed, yielding B_0'' = 0.160 35 ± 0.000 07 cm^{-1}. The corresponding bond length for $^{27}Al^{59}Co$ is r_0'' = 2.3833 ± 0.0005 Å.

Rotationally resolved spectra for AlV were also recorded although the results are less definitive. As described in Sec. III A, the low resolution spectrum of AlV is very dense extending far into the infrared energy regime. In order to locate discrete vibronic bands suitable for high resolution study it was necessary to scan energies in the 8000–10 000 cm^{-1} range. Performing rotational analyses in this energy regime necessitates the use of the H_2 Raman shifter in a configuration such that the Stokes radiation is used to interrogate the molecular beam, the weaker anti-Stokes radiation is used to collect the I_2 spectrum for calibration purposes, and the highest power fundamental radiation must be filtered out to prevent complications associated with two laser frequencies being admitted into the I_2 cell and monitor étalons. Although high resolution studies of over one dozen vibronic bands were attempted, only three spectra were successfully fit. The rotational line positions of all three rotationally analyzed bands can be found in Table II.

Figure 7 displays the 9074 cm^{-1} band of $^{27}Al^{51}V$, which is characterized by an intense R branch with an R bandhead, a weaker Q branch, and a weak P branch. This intensity pattern is characteristic of $\Delta\Omega=+1$ transitions, so possibilities of $\Omega'=1\leftarrow\Omega''=0$, $\Omega'=2\leftarrow\Omega''=1$, $\Omega'=3\leftarrow\Omega''=2$, etc.

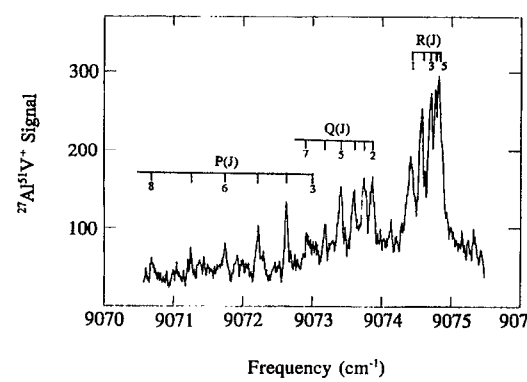

FIG. 7. High resolution scan over the 9074 cm^{-1} band in $^{27}Al^{51}V$. This band is fit as an $\Omega'=2\leftarrow\Omega''=1$ transition in which the bond lengthens upon excitation as is suggested by the bandhead in the R branch.

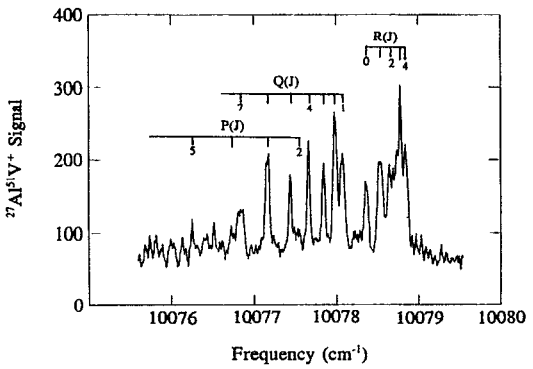

FIG. 8. Rotationally resolved scan over the 10 078 cm^{-1} band in $^{27}Al^{51}V$. In contrast to the 9074 cm^{-1} band, this band is fit as a $\Omega'=1\leftarrow\Omega''=0$ transition, indicating that the transition originates from a different electronic state that is populated in the molecular beam. The $\Omega''=0$ state is thought to be the true ground state of the molecule while the $\Omega'=1$ state is believed to be an excited spin–orbit component of the ground state.

were considered for the transition. The only reasonable fit to Eq. (3.3) was obtained for the $\Omega'=2\leftarrow\Omega'=1$ assignment, resulting in rotational constants for $^{27}Al^{51}V$ of $B'=0.118\ 62\pm0.000\ 42$ cm^{-1} and $B_0''=0.137\ 68\pm0.000\ 34$ cm^{-1}.

Two of the other high resolution spectra of AlV could be analyzed. These were the bands at 10 078 and 9081 cm^{-1}, which are displayed in Figs. 8 and 9, respectively. Both of these transitions again have bandheads in the R branch, indicative of a bond lengthening upon electronic excitation and both can be fit as $\Omega'=1\leftarrow\Omega''=0$ transitions. The 10 078 cm^{-1} band displays a rather low signal-to-noise ratio, but can nevertheless be fitted very well by the standard formula presented in Eq. (3.3), yielding a ground state rotational constant of $B_0''=0.139\ 34\pm0.000\ 44$ cm^{-1}. On the other hand, the 9081 cm^{-1} band displayed in Fig. 8 was difficult to fit and the lower state rotational constant obtained reflects this difficulty in a larger error limit, with $B_0''=0.139\ 07\pm0.000\ 82$ cm^{-1}. The spectrum could be successfully fit only upon inclusion of lambda doubling in the upper state. Once the fit was obtained, a rotational simulation of the band was performed and the most striking difference between the experimental data and the simulation was the unexplainable lack of intensity in the Q branch lines. In addition, the highest $P(J)$ lines could not be fit unless considered as high $Q(J)$ lines; accordingly the $P(7)$ and $P(8)$ line positions were excluded from the fit. The spectrum presented in Fig. 8 is a summation of four individual scans. Close examination of the individual scans showed that the apparent $P(7)$ line was prominent in only one scan, where it displayed an anomalously large intensity. It is therefore possible that this feature is an artifact of some sort. In any event, the assignment reported in Table II is the most reasonable one that we can derive.

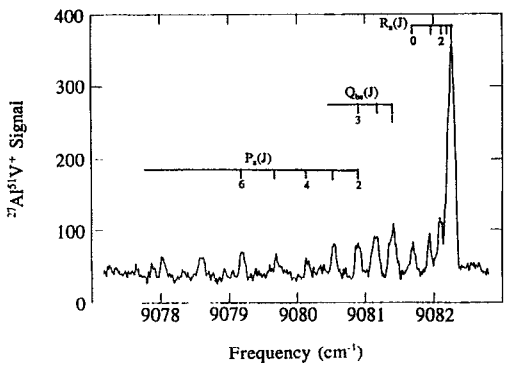

FIG. 9. High resolution scan over the 9081 cm^{-1} $\Omega'=1\leftarrow\Omega''=0$ transition in diatomic $^{27}Al^{51}V$. A reasonable rotational fit of this band could be obtained only upon inclusion of a lambda doubling parameter in the upper state yielding values of $B_0'=0.102\ 79\pm0.001\ 18$ cm^{-1}, $B_0''=0.139\ 07\pm0.000\ 82$ cm^{-1}, and $q'=-0.030\ 38\pm0.001\ 72$ cm^{-1}.

The similarity of the three measured lower state rotational constants suggests that the two different Ω'' values observed, $\Omega''=0$ and 1, correspond to two different spin–orbit levels of the same Hund's case (a) molecular ground state, and that complete quenching of the spin–orbit levels has not been achieved in the molecular beam. This idea will be discussed further in Sec. IV C below. The rotational constant reported for the ground state $\Omega''=0$ level is a weighted least squares combination of the rotational constants obtained upon fitting the 9081 and 10 078 cm^{-1} bands, providing $B_0''=0.139\ 28\pm0.000\ 39$ cm^{-1} and $r_0''=2.6195\pm0.0036$ Å.

IV. DISCUSSION

Previous work[1–4] performed in this group on the $3d$ transition metal aluminides has been successful in characterizing the favored approach of the Al atom to the transition metal as $3p\sigma$ or $3p\pi$, depending on whether a $3d^{n+1}4s^1$ configuration is accessible or not. This work was unsuccessful in addressing the question of $3p\pi_{Al}$–$3d\pi_M$ bonding in these species, however. In AlNi, AlCu, and AlZn it is believed that the contracted nature of the $3d$ orbitals makes them inaccessible for bonding with the aluminum $3p$ orbital. In the case of AlCa, theoretical studies showed little evidence of $3p\pi_{Al}$–$3d\pi_{Ca}$ contributions to the bonding.[3] In contrast, studies of the open $3d$-subshell transition metal aluminides, particularly those originating from the left-hand side of the $3d$ series where the $3d$ orbitals may indeed be large enough for bonding interactions to occur, may shed some light on the possibility of significant $3p\pi_{Al}$–$3d\pi_M$ bonding.

Experimental elucidation of the chemical bonding in diatomic molecules requires the determination and comparison of various experimental observables, particularly the bond length, bond strength, and vibrational frequency of the ground state of the molecule. The bond strength provides a starting point for this analysis, although the question of which separated atom limit leads to the ground state of the molecule can cloud the interpretation. It has been shown, for example, that for diatomic transition metals formed from atoms with d^ms^2 ground states, promotion to the excited $d^{m+1}s^1$ atomic state generally results in a strong s-based σ^2 chemical bond. In the diatomic transition metals, however, consideration must be given to the singly promoted

$s\sigma^2 d^m d^{n+1} s\sigma^{*1}$ or $s\sigma^2 d^{m+1} d^n s\sigma^{*1}$ configurations as well as to the doubly promoted $s\sigma^2 d^{m+1} d^{n+1}$ configuration, because in some examples the energy gained by the formation of a favorable $s\sigma^2$ bond is insufficient to make up for the energetic costs of preparing both atoms for bonding.

Consideration of the appropriate separated atom limits is considerably simplified in the case of the transition metal aluminides because the $3s^2 3p^1, {}^2P^0$ ground state aluminum atom in its $3p\sigma$ orientation already behaves similarly to the $d^{m+1}s^1$ states of the transition metal atoms: it is capable of forming a strong σ^2 bond with a transition metal having a single s electron, as has been demonstrated for AlCu[2] and AlNi.[1] Thus, only promotion of the transition metal atom need be considered. In the present study we define the promotion energy of a transition metal atom to be the amount of energy required to excite the atom from its ground state to the lowest energy state deriving from a $d^{m+1}s^1$ configuration. Finally, we define the intrinsic bond strength of the molecule as the measured bond strength plus the energy required to prepare the atoms for bonding, assuming that the bond arises from the lowest Al $(3s^2 3p^1, {}^2P^0)$+M $(3d^{m+1}4s^1)$ separated atom limit. The intrinsic bond strength thus provides an estimate of what the bond strength would be if it were not necessary to promote the transition metal to an excited electronic state in preparation for bonding.

The ground state bond length of a diatomic molecule, as measured through rotational analysis of a spectrum, can also be useful in considering various possible types of bonding interactions. In addition, molecular state symmetries determined through the analysis of rotationally resolved data can preclude certain ground electronic state configurations while supporting others. By combining different pieces of the molecular puzzle and then comparing one transition metal aluminide with the next it has been possible in these studies to establish that $3d\pi$–$3p\pi$ bonding does indeed contribute to the chemical bonding in the AlM molecules to some degree.

A. AlCr

In the open $3d$-subshell transition metal aluminides the chemical bonding in the ground state of the molecule depends on the balance between the energy gained by the formation of a σ^2 bond versus the energetic cost associated with promoting the transition metal atom in preparation for bonding. In the simplest case, that found in AlCr, the work described above provides a bond strength of $D_0^0(\mathrm{AlCr})=2.272\pm0.009$ eV. In the AlCr molecule the ground separated atom limit of Al $(3s^2 3p^1, {}^2P^0)$+Cr $(3d^5 4s^1, {}^7S)$ allows the formation of a strong $(3p\sigma$–$4s\sigma)$ σ^2 bond without the expenditure of energy to prepare the atoms for bonding. Therefore 2.272 ± 0.009 eV also represents the intrinsic bond strength of the AlCr molecule.

Only four Hund's case (a) states result from the ground separated atom limit of Al $(3s^2 3p^1, {}^2P^0)$+Cr $(3d^5 4s^1, {}^7S)$: ${}^6\Sigma^+$, ${}^6\Pi$, ${}^8\Sigma^+$, and ${}^8\Pi$. These correspond to couplings of the $4s_{\mathrm{Cr}}$ and $3p_{\mathrm{Al}}$ electrons of σ^2 $({}^1\Sigma^+)$, $\sigma^1\pi^1$ $({}^1\Pi)$, $\sigma^1\sigma^{*1}$ $({}^3\Sigma^+)$, and $\sigma^1\pi^1$ $({}^3\Pi)$, respectively, and may be expected to fall in the energetic ordering: $3s^2_{\mathrm{Al}}3d^5_{\mathrm{Cr}}({}^6S)\sigma^2$, ${}^6\Sigma^+ < 3s^2_{\mathrm{Al}}3d^5_{\mathrm{Cr}}({}^6S)\sigma^1\pi^1$, ${}^8\Pi < 3s^2_{\mathrm{Al}}3d^5_{\mathrm{Cr}}({}^6S)\sigma^1\pi^1$, ${}^6\Pi < 3s^2_{\mathrm{Al}}3d^5_{\mathrm{Cr}}({}^6S)\sigma^1\sigma^{*1}$, ${}^8\Sigma^+$ assuming insignificant $3d\pi_{\mathrm{Cr}}$–$3p\pi_{\mathrm{Al}}$ contributions to the chemical bonding (if π bonding interactions are significant the order of the ${}^8\Pi$ and ${}^6\Pi$ states may be reversed). The ground state is thus expected to be ${}^6\Sigma^+$, although at present no experimental proof exists. In this molecule the chemical bonding is expected to be dominated by the σ^2 bond, so it should come as no surprise that the intrinsic bond strength of AlCr (2.272 ± 0.009 eV) is similar to the intrinsic bond strengths of AlNi (2.32 ± 0.05 eV)[1] and AlCu (2.315 ± 0.012 eV).[2]

B. AlCo

The onset of predissociation in AlCo yields a ground state dissociation energy of 1.844 ± 0.002 eV. Assuming that the ground state of AlCo derives from the combination of a ground state Al $(3s^2 3p^1, {}^2P^0)$ atom interacting with a promoted Co $[3d^8({}^3F)4s^1, {}^4F]$ atom, an intrinsic bond strength of 2.276 ± 0.002 eV is obtained. This intrinsic bond strength is again typical of a two electron σ^2 bond as found in AlNi (2.32 ± 0.05 eV),[1] AlCu (2.315 ± 0.012 eV),[2] and AlCr (2.272 ± 0.009 eV), suggesting strongly that the AlCo ground state does derive from the interaction of Al $(3s^2 3p^1, {}^2P^0)$+Co $[3d^8({}^3F)4s^1, {}^4F]$. Accordingly the AlCo ground state may be described as deriving from the $3s^2_{\mathrm{Al}}3d^8_{\mathrm{Co}}({}^3F)\sigma^2$ configuration.

Whereas in AlCr there existed only four Hund's case (a) states deriving from the appropriate separated atom limit, in AlCo many more states derive from the Al $(3s^2 3p^1, {}^2P^0)$+Co $[3d^8({}^3F)4s^1, {}^4F]$ limit. Restricting ourselves to only those states which can arise from the configuration which has the favorable σ^2 bond $[3s^2_{\mathrm{Al}}3d^8_{\mathrm{Co}}({}^3F)\sigma^2]$, leads to possible ground states of ${}^3\Phi_i$, ${}^3\Delta_i$, ${}^3\Pi_i$, and ${}^3\Sigma^-$. The lowest Ω levels expected for these Hund's case (a) states would be $\Omega=4$ $({}^3\Phi_i)$, $\Omega=3$ $({}^3\Delta_i)$, $\Omega=2$ $({}^3\Pi_i)$, and $\Omega=0^+$ or 1 $({}^3\Sigma^-)$. The experimental observation of an $\Omega=3$ ground state then identifies the ground state of AlCo as ${}^3\Delta_3$.

The $3s^2_{\mathrm{Al}}3d^9_{\mathrm{Ni}}\sigma^2$, ${}^2\Delta_{5/2}$ ground state found for AlNi was in agreement with the results of a simple ligand-field plus spin–orbit model[28] in which the tenfold degeneracy of the $3d^9$ core of nickel was split by the electrostatic field of the Al atom (which carried an effective positive charge) and spin–orbit effects. However, this model predicts a ${}^3\Phi_4$ ground state as the lowest energy state deriving from the $3s^2_{\mathrm{Al}}3d^8_{\mathrm{Co}}({}^3F)\sigma^2$ configuration of AlCo, in contrast to the experimental results. In essence, this model favors a ${}^3\Phi_i$ ground state because in a positive ligand field as expected for aluminum, the $3d_{\mathrm{Co}}$ orbitals will fall in the order $3d\sigma < 3d\pi < 3d\delta$, leading to a ground molecular configuration of $3s^2_{\mathrm{Al}}3d\sigma^2_{\mathrm{Co}}3d\pi^3_{\mathrm{Co}}3d\delta^3_{\mathrm{Co}}\sigma^2$, ${}^3\Phi_i$.

An alternative to the ligand field model for the energetic ordering of the $3d$ orbitals is a molecular orbital model. In this model a bonding interaction between the $3d\pi_{\mathrm{Co}}$ and $3p\pi_{\mathrm{Al}}$ orbitals is hypothesized, leading to an expected energy ordering of $\pi < 3d\sigma \approx 3d\delta < \pi^*$, where the π orbital is expected to be primarily $3d\pi_{\mathrm{Co}}$ in character and the π^* orbital is primarily $3p\pi_{\mathrm{Al}}$ in character. Filling these orbitals in order with the eight remaining electrons and maintaining the

triplet coupling required by the $3d^8(^3F)4s^1$, ^4F state of the promoted cobalt atom will then lead to a ground configuration of either $3s^2_{Al}\pi^4 3d\delta^3 3d\sigma^1\sigma^2$, $^3\Delta_i$ if the $3d\delta$ orbital lies lower in energy than the $3d\sigma$ orbital or $3s^2_{Al}\pi^4 3d\sigma^2 3d\delta^2\sigma^2$, $^3\Sigma^-$ if the $3d\sigma$ orbital lies lower in energy than the $3d\delta$ orbital.

The observation of $\Omega=3$ as the ground level of AlCo identifies the $3s^2_{Al}\pi^4 3d\delta^3 3d\sigma^1\sigma^2$, $^3\Delta_i$ state as the ground state and suggests that the $3d\delta$ orbital lies lower in energy than the $3d\sigma$ orbital, again contradicting the results of the ligand field model. However, there is an important reason why the $3s^2_{Al}\pi^4 3d\sigma^2 3d\delta^2\sigma^2$, $^3\Sigma^-$ state should lie above the $3s^2_{Al}\pi^4 3d\delta^3 3d\sigma^1\sigma^2$, $^3\Delta_i$ state even in the ligand field model. The $3s^2_{Al}\pi^4 3d\sigma^2 3d\delta^2\sigma^2$, $^3\Sigma^-$ state does not represent a pure ^3F coupling of the two $3d$ holes on cobalt, but instead corresponds to a state which is 20% $3d^8$, ^3F, and 80% $3d^8$, ^3P in character. Because the $3d^8$, ^3P state of the highly contracted Co^+ ion is strongly disfavored by exchange effects, it lies roughly 13 000 cm^{-1} above the $3d^8$, ^3F ground state. The admixture of 80% of the exchange-disfavored $3d^8$, ^3P wave function into the $3s^2_{Al}\pi^4 3d\sigma^2 3d\delta^2\sigma^2$, $^3\Sigma^-$ state effectively removes it from contention as the ground state in this molecule. On the other hand, the $3s^2_{Al}\pi^2 3d\sigma^2 3d\delta^4\sigma^2$, $^3\Sigma^-$ state is 80% $3d^8$, ^3F, and 20% $3d^8$, ^3P in character, making it somewhat favored by exchange effects. However, this state only places two electrons in the π orbital that is conjectured to have bonding character between the aluminum and the cobalt, and therefore cannot effectively compete against the $3s^2_{Al}\pi^4 3d\delta^3 3d\sigma^1\sigma^2$, $^3\Delta_i$ state as a candidate for the ground state.

Another factor which can influence the energy ordering of the molecular orbitals is the possibility of $4s\sigma-3d\sigma$ hybridization in the cobalt atom. Orbital mixing of this type can make the "$3p\sigma_{Al}-4s\sigma_{Co}$" bonding orbital of AlCo more strongly bonding at the expense of moving the "$3d\sigma$" orbital higher in energy. Such effects have been suggested in the example of Ti_2, where the ground state has been experimentally shown to be $4s\sigma_g^2 3d\pi_u^4 3d\sigma_g^1 3d\delta_g^1$, $^3\Delta_g$.[29] Evidence for $4s\sigma-3d\sigma$ hybridization in AlCo may be found in the large hyperfine splitting of the ground state.

As mentioned in Sec. III C, diatomic AlCo appears to have a rather large hyperfine interaction in the ground state, with $(2a+b+c)\approx 0.04$ cm^{-1}. In most examples of molecules having significant hyperfine interactions, the hyperfine splitting is dominated by the Fermi contact interaction, which arises because of the finite possibility of an unpaired electron reaching the spatial coordinates of the nucleus. This can only occur for s orbitals, however, because they are the only atomic orbitals having amplitude at the nucleus. The existence of a rather large hyperfine splitting in AlCo may therefore be taken as evidence that the $3d\sigma$ orbital in the $3s^2_{Al}\pi^4 3d\delta^3 3d\sigma^1\sigma^2$, $^3\Delta_i$ ground state has taken on some $4s_{Co}$ character, thereby considerably increasing the Fermi contact interaction with the ^{59}Co nucleus. It would be very interesting to investigate this possibility further by resolving the hyperfine structure of the low-J lines in the spectrum of Fig. 5, but this is beyond our present experimental capabilities.

Although the possibility of $3d\pi_{Co}-3p\pi_{Al}$ bonding interactions seemed rather unlikely in our initial consideration of this molecule, it now seems that this is indeed occurring to some degree. In this context we note that the increased size of the $3d$ orbitals in cobalt as compared to nickel causes greater d-orbital contributions to the bond strengths of YCo, ZrCo, and NbCo as compared to YNi, ZrNi, and NbNi.[9] This supports the possibility that $3d\pi-3p\pi$ bonding becomes appreciable in the transition metal aluminides as one moves from nickel to cobalt in the $3d$ transition metal series. Thus, the determination of the ground state symmetry of AlCo has provided the first evidence of $3d\pi-3p\pi$ bonding in the transition metal aluminides.

C. AlV

The promotion energy required to prepare vanadium in its $3d^4(^5D)4s^1$, $^6D_{1/2}$ state (which is ideally set up for formation of a $3p\sigma_{Al}-4s\sigma_V$ bond with aluminum) is only 2112 cm^{-1}.[20] This is considerably less than the promotion energy of 3483 cm^{-1} that was required to prepare the cobalt atom in the $3d^8(^3F)4s^1$, $^4F_{9/2}$ state that correlates with the ground state of AlCo.[20] Accordingly, we expect the ground state of AlV to result from the interaction of a promoted $3d^4(^5D)4s^1$, $^6D_{1/2}$ vanadium atom with a ground state $3s^2 3p^1$, $^2P^0$ aluminum atom. The measured dissociation energy of AlV is only 1.489 ± 0.010 eV, providing an intrinsic bond strength of 1.751 ± 0.010 eV. This value is reduced significantly from the intrinsic bond strengths of other transition metal aluminides which are bonded primarily by $3p\sigma_{Al}-4s\sigma_M$ σ^2 bonds, such as AlNi (2.32 ± 0.05 eV),[1] AlCu (2.315 ± 0.0012 eV),[2] AlCr (2.272 ± 0.009 eV), and AlCo (2.276 ± 0.002 eV). At the present time we do not understand why the AlV bond is so anomalously weak.

Assuming that the high spin coupling of the $3d$ electrons is retained, the combination of a ground state $3s^2 3p^1$, $^2P^0$ aluminum atom with a promoted $3d^4(^5D)4s^1$, $^6D_{1/2}$ vanadium atom leads to $3s^2_{Al}3d\delta^1_V 3d\pi^2_V 3d\sigma^1_V\sigma^2$, $^5\Delta_r$, $3s^2_{Al}3d\delta^2_V 3d\pi^1_V 3d\sigma^1_V\sigma^2$, $^5\Pi_r$, and $3s^2_{Al}3d\delta^2_V 3d\pi^2_V\sigma^2$, $^5\Sigma^+$ states having the favorable $3p\sigma_{Al}-4s\sigma_V$ σ^2 bond. The identification of the AlCo ground state as $^3\Delta_i$ demonstrated the existence of a $3p\pi_{Al}-3d\pi_{Co}$ bonding interaction which lowers the orbital energy of the $3d\pi$ orbitals, so on this basis one would expect the ground state of AlV to be either $3s^2_{Al}\pi^2 3d\delta^1_V 3d\sigma^1_V\sigma^2$, $^5\Delta_r$ or $3s^2_{Al}\pi^2 3d\delta^2_V\sigma^2$, $^5\Sigma^+$, depending on the relative energy orderings of the $3d\sigma$ and $3d\delta$ orbitals. The $^5\Delta_r$ state will have spin–orbit levels falling in the order $\Omega=4>\Omega=3>\Omega=2>\Omega=1>\Omega=0^+\approx\Omega=0^-$, while the $^5\Sigma^+$ state is expected to have spin–orbit levels of $\Omega=2$, $\Omega=1$, and $\Omega=0^+$. In the latter case it is likely that the spin–orbit levels will fall in the energetic ordering $\Omega=2>\Omega=1>\Omega=0^+$, assuming that the dominant cause of the splitting is second-order spin–orbit interaction with the higher energy $3s^2_{Al}3d\delta^2_V 3d\pi^1_V 3d\sigma^1_V\sigma^2$, $^5\Pi_r$ state. In either case the ground level is expected to be an $\Omega=0$ level, with an $\Omega=1$ level lying somewhat higher in energy. [If the ground state is $^5\Delta_r$, it may be readily demonstrated that the $^5\Delta_1-^5\Delta_0$ interval is expected to be $\zeta_{3d}/2$, which is approximately 88 cm^{-1}.[30] If the ground state is $^5\Sigma^+$ the

$^5\Sigma_1^+ - {}^5\Sigma_{0+}^+$ interval is expected to be $3\zeta_{3d}^2/16T(^5\Pi_r)$, where ζ_{3d} is the spin–orbit parameter for a $3d$ orbital of vanadium and $T(^5\Pi_r)$ is the energy of the $^5\Pi_r$ state above the ground state.] Since lower state levels with both $\Omega''=0$ and 1 have been identified in the rotationally resolved work, it is impossible at this time to determine whether the ground state of AlV is $3s_{\mathrm{Al}}^2\pi^2 3d\delta_{\mathrm{V}}^1 3d\sigma_{\mathrm{V}}^1\sigma^2$, $^5\Delta_r$ or $3s_{\mathrm{Al}}^2\pi^2 3d\delta_{\mathrm{V}}^2\sigma^2$, $^5\Sigma^+$.

In addition to the anomalous bond strength noted above for AlV, the bond length [$r_0''(\mathrm{AlV})=2.620\pm0.004$ Å] is also anomalously long compared to the other transition metal aluminides that are thought to possess the favorable $3p\sigma_{\mathrm{Al}}$–$4s\sigma_{\mathrm{M}}$ σ^2 bond [$r_0''(\mathrm{AlCu})=2.3389\pm0.0004$ Å;[2] $r_0''(\mathrm{AlNi})=2.3211\pm0.0007$ Å;[1] and $r_0''(\mathrm{AlCo})=2.3833\pm0.0005$ Å]. The increased bond length of AlV is not as anomalous as it might first appear, however. In comparing the expectation values of $\langle r\rangle$ for the $4s$ orbitals of Cu, Ni, Co, Cr, and V, calculated for the $3d^{n+1}4s^1$ configurations by numerical Hartree–Fock methods[31] (and corrected for relativistic effects by the ratios of the relativistic values to the nonrelativistic ones)[32] we find that the values for Ni, Co, and V are increased from that reported for Cu by 0.028, 0.062, and 0.271 Å, respectively. In comparison, the measured bond lengths of AlNi, AlCo, and AlV exceed that of AlCu by −0.018, +0.044, and +0.281 Å, respectively. Thus the bond length of AlV is indeed consistent with the notion that promotion of the vanadium atom to the $3d^4(^5D)4s^1$, ^6D state, followed by formation of a two-electron $3p\sigma_{\mathrm{Al}}$–$4s\sigma_{\mathrm{V}}$ σ^2 bond is occurring.

V. CONCLUSION

Resonant two-photon ionization spectroscopy has been employed to characterize the chemical bonding in three diatomic transition metal aluminides, AlV, AlCr, and AlCo. All three species are thought to chemically bond through the formation of a covalent bond between a single $4s$ electron on the transition metal atom and a single $3p\sigma$ electron on the aluminum atom. Diatomic AlCr is assumed to have an $X\ ^6\Sigma^+$ ground state, and the dissociation energy has been measured by the onset of predissociation in a dense set of vibronic levels as $D_0^0(\mathrm{AlCr})=2.272\pm0.009$ eV. The ground state of AlCo has been determined to be $X\ ^3\Delta_i$, with a bond length of 2.3833 ± 0.0005 Å, and a bond strength of $D_0^0(\mathrm{AlCo})=1.844\pm0.002$ eV. In contrast to these results, AlV exhibits an unusually low bond strength of $D_0^0(\mathrm{AlV})=1.489\pm0.010$ eV, and a longer bond length of $r_0''(\mathrm{AlV})=2.620\pm0.004$ Å. Ionization energies were also measured for all three species, and $d\pi$–$p\pi$ bonding interactions were inferred from the $^3\Delta_i$ ground state of AlCo.

ACKNOWLEDGMENTS

We are grateful to Caleb A. Arrington for his skillful preparation of the metal alloy samples used in this spectroscopic investigation and for the construction of the Raman shifting apparatus used to Stokes shift the excimer laser radiation. We also gratefully acknowledge research support from the National Science Foundation under Grant No. CHE-9215193. Acknowledgment is also made to the donors of the Petroleum Research Fund, administered by the American Chemical Society for partial support of this research. J. M. B. expresses sincere gratitude to the Eastman Kodak Company for supplying her with a predoctoral fellowship.

[1] J. M. Behm, C. A. Arrington, and M. D. Morse, J. Chem. Phys. **99**, 6409 (1993).
[2] J. M. Behm, C. A. Arrington, J. D. Langenberg, and M. D. Morse, J. Chem. Phys. **99**, 6394 (1993).
[3] J. M. Behm, M. D. Morse, A. I. Boldyrev, and J. Simons, J. Chem. Phys. **101**, 5441 (1994).
[4] J. M. Behm, T. Blume, and M. D. Morse, J. Chem. Phys. **101**, 5454 (1994).
[5] J. C. Pinegar, J. D. Langenberg, C. A. Arrington, E. M. Spain, and M. D. Morse, J. Chem. Phys. (submitted).
[6] Z.-W. Fu and M. D. Morse, J. Chem. Phys. **90**, 3417 (1989).
[7] M. D. Morse, Adv. Metal Semiconductor Clusters **1**, 83 (1993).
[8] Z.-W. Fu, G. W. Lemire, Y. Hamrick, S. Taylor, J.-C. Shui, and M. D. Morse, J. Chem. Phys. **88**, 3524 (1988).
[9] C. A. Arrington, T. Blume, M. D. Morse, M. Doverstål, and U. Sassenberg, J. Phys. Chem. **98**, 1398 (1994).
[10] Z.-W. Fu, G. W. Lemire, G. A. Bishea, and M. D. Morse, J. Chem. Phys. **93**, 8420 (1990).
[11] E. M. Spain and M. D. Morse, J. Phys. Chem. **92**, 2479 (1992).
[12] K. Hilpert and K. Ruthardt, Ber. Bunsenges. Phys. Chem. **91**, 724 (1987).
[13] I. Shim and K. A. Gingerich, J. Chem. Phys. **78**, 5693 (1983).
[14] T. R. Loree, R. C. Sze, and D. L. Barker, Appl. Phys. Lett. **31**, 37 (1977).
[15] D. J. Clouthier and J. Karolczak, Rev. Sci. Instrum. **61**, 1607 (1990).
[16] S. Gerstenkorn and P. Luc, *Atlas du Spectre d'Absorption de la Molécule d'Iode: 14 800–20 000 cm^{-1}* (CNRS, Paris, 1978); S. Gerstenkorn and P. Luc, Rev. Phys. Appl. **14**, 791 (1979).
[17] P. R. Bevington, *Data Reduction and Error Analysis for the Physical Sciences* (McGraw–Hill, New York, 1969), CURFIT program, p. 235.
[18] L. M. Russon, S. A. Heidecke, M. K. Birke, J. Conceicao, M. D. Morse, and P. B. Armentrout, J. Chem. Phys. **100**, 4747 (1994).
[19] L. M. Russon, S. A. Heidecke, M. K. Birke, J. Conceicao, P. B. Armentrout, and M. D. Morse, Chem. Phys. Lett. **204**, 2350 (1993).
[20] C. E. Moore, *Atomic Energy Levels*, Natl. Bur. Stand. U.S. Circ. No. 467 (U.S. GPO, Washington, DC, 1971).
[21] E. S. Chang, J. Phys. Chem. Ref. Data **19**, 119 (1990).
[22] R. H. Page and C. S. Gudeman, J. Opt. Soc. Am. B **7**, 1761 (1990); A. M. James, P. Kowalczyk, E. Langlois, M. D. Campbell, A. Ogawa, and B. Simard, J. Chem. Phys. **101**, 4485 (1994).
[23] J. Sugar and C. Corliss, J. Phys. Chem. Ref. Data **6**, 317 (1977).
[24] J. Sugar and C. Corliss, J. Phys. Chem. Ref. Data **10**, 1097 (1981).
[25] C. H. Townes and A. L. Schawlow, *Microwave Spectroscopy* (McGraw–Hill, New York, 1955).
[26] T. M. Dunn, in *Molecular Spectroscopy: Modern Research*, edited by K. N. Rao and C. W. Matthews (Academic, New York, 1972), pp. 231–257.
[27] W. Weltner, Jr., *Magnetic Atoms and Molecules* (Dover, New York, 1983), p. 346.
[28] E. M. Spain and M. D. Morse, J. Chem. Phys. **97**, 4641 (1992).
[29] M. Doverstål, B. Lindgren, U. Sassenberg, C. A. Arrington, and M. D. Morse, J. Chem. Phys. **97**, 7087 (1992).
[30] H. Lefebvre-Brion and R. W. Field, *Perturbations in the Spectra of Diatomic Molecules* (Academic, Orlando, FL, 1986).
[31] C. W. Bauschlicher, Jr. (personal communication).
[32] J. P. Desclaux, At. Data Nucl. Data Tables **12**, 311 (1973).